Enhancing the dynamic frequency of microgrids by means of PV power plants with integrated energy storage

Daniel Munteanu, Ioan Serban, Corneliu Marinescu, Luminita Barote
Department of Electrical Engineering and Applied Physics, Transilvania University of Brasov, Brasov, Romania
Email: munteanu.d@unitbv.ro

Abstract - **Achieving[1] a high-level of stability represents one major concern in autonomous microgrids (MGs) with high penetration levels of renewable energy sources. The aim of this paper is to study how photovoltaic (PV) power plants can provide dynamic frequency support in MGs, in order to obtain an improved stability for the entire power system. On the PV side an energy storage subsystem is added, with the main purpose of better control and higher power reserve of the PV power plant. By this way the necessary input power is provided by the PV system along with the battery block. The required output power is supplied by a three-phase voltage source converter (VSC). The VSC control is implemented in a rotating *dq* reference frame, including a harmonic compensation loop for the output current. To improve the dynamic frequency stability of the MG, specific functions are implemented within the PV inverter control. To highlight the performance of the proposed system, a comparative analysis is provided, which cover four cases of interest depending on the status of the storage system and dynamic support (i.e. with/without storage and with/without dynamic support). Simulation results are included to validate the power control system, showing that the dynamic frequency control can be improved by the proposed solution.**

Keywords: *Frequency control; microgrid; power system dynamic stability; PV power generation, energy storage.*

I. INTRODUCTION

The rapid development growth of distributed generation systems is mainly associated with the sector of Renewable Energy Sources (RES). Aiming to maximize the use of local energy resources as close as possible to the consumers and to reduce the losses on the conventional networks have led to the necessity of developing small self-sustaining power systems, namely microgrids (MGs) [1]. Moreover, the MG is considered the building block in the future smart grid [2]. The automated MGs will take the control of the power systems related to the stability of supply and energy quality, mainly because the exponential increase of the control complexity makes no longer possible the human dispatcher to perform it. Within this framework, the RES-base generators should also have to participate to ensuring the MG power quality and stability. Therefore, the main tasks have to be shared among all the resources in the MG, sources, energy storage systems and consumers [3].

[1] This work was supported by a grant of the Romanian National Authority for Scientific Research and Innovation, CNCS – UEFISCDI, project number PN-II-RU-TE-2014-4-0359.

A major issue of the grids with high RES penetration levels consists in ensuring the power control and predictability. In this regard, the RES generators must become controllable in a similar way to conventional ones. In autonomous MGs, maintaining the stability both in normal operating conditions and during severe dynamic regimes represents a more difficult task mainly because of its reduced inertia and power reserve [19]. Therefore, besides enhancing the MG stability and power availability by means of energy storage systems and active loads, improving the RES generators control mainly during dynamic regimes represents a new real concern.

The current research is focused on the photovoltaic (PV) source, because of its high potential in terms of answer speed capability to face with the stability problems, part of which are created in large extent by its own inherent variability of energy production. The premise used to date, consisting in maximising the energy production using a maximum power point tracking (MPPT) algorithm, will be replaced by the higher priority request to participate to the MG operational stability. The main studied solutions to achieve a more flexible power control of PV power plants consist in integrating energy storage systems within the power plant structure [4]-[7], curtailing the PV output power to a certain degree [8]-[11], or combination of both solutions. Although such solutions increase the costs – either in terms of additional resources (e.g. energy storage system), or because of not using the entire available solar energy when operating outside the maximum power point – they are justified when ensuring the security and stability in MGs with limited resources becomes a priority.

Integrating an energy storage system within a PV power plant to enhance its power control can be accomplished in several ways. The solution of interest for the current study involves connecting a battery bank to the DC-link of the PV inverter by means of a bidirectional DC-DC converter [13], [15]. To be mentioned that this paper is an extension of a previous study [20], being mainly focused on the operation strategy and control of the PV-battery system in order to increase the active power control of the PV power plant and thus, to be able to participate in the MG dynamic frequency control mechanism [12]-[14],[16].

After introduction, the paper is organized as follows: Section II presents the three-phase inverter (VSC) and system configuration, in Section III the control principle and control methods of the VSC are detailed, Section IV describes the simulation cases and results while the main conclusions are provided in Section V.

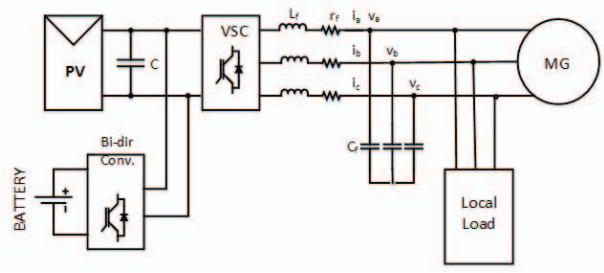

Fig.1. Block diagram of the analysed system

II. PV System Configuration

Fig. 1 shows the block diagram of the studied PV system, consisting of a three-phase VSC connected to a MG. The inverter is supplied from a PV system and a battery block is connected on the DC-link to support either a local load connected when operating islanded, or to provide dynamic support when connected to the MG.

The analysed PV power plant consists in a single string with 22 series connected panels each having 245 W. The PV string is connected directly to the VSC DC-link, the rated DC voltage produced by the string being around 650V.

A 48V battery is connected to the VSC DC-link by means of a DC-DC bidirectional converter. It should be mentioned that the discussion about the converter structure and its impact on the overall system efficiency are issues outside the focus of the current paper and, therefore, a generic DC-DC half-bridge converter is considered. Another important aspect that is reserved for future studies implies the optimization of the converter power and battery capacity. If the PV system is intended to support the MG only during severe dynamic regimes, a short-term energy storage system is to be considered.

III. System Control

A. VSC Power control

The control of the VSC output power is accomplished in rotating *dq* reference frame, with the block diagram developed as in Fig. 2a and Fig. 2b. The inner current loop is based on proportional-integrator (PI) controllers on each axis, with voltage feed-forward and cross-coupling elimination terms [17]. The synchronization of the inverter is done by a conventional three-phase phase-locked loop (PLL). Based on the active and reactive power references (P_{PV}^*, Q_{PV}^*), the *dq*-axis reference currents are calculated as follows [17]:

$$I_d^* = \frac{2}{3}\frac{P_{PV}^* V_d + Q_{PV}^* V_q}{V_d^2 + V_q^2} \quad (1)$$

$$I_q^* = \frac{2}{3}\frac{P_{PV}^* V_q - Q_{PV}^* V_d}{V_d^2 + V_q^2} \quad (2)$$

For limiting the output current distortion to the standard level (i.e. $THD_I < 5\%$), the VSC control also includes a harmonic compensation (HC) loop, presented in Fig. 2c. The HC is implemented in rotating reference frames, one for each harmonic that is required to be compensated. In this case, targeting for the 5th and 7th harmonics, two

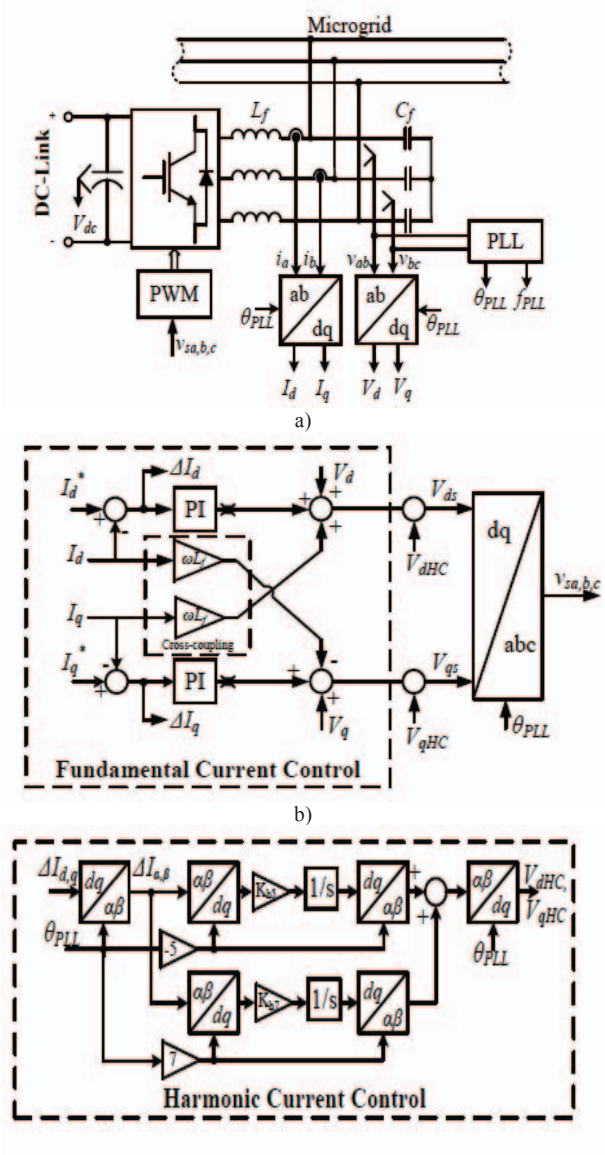

Fig.2. VSC command: a) general structure; b) fundamental current control diagram; c) harmonic current control diagram

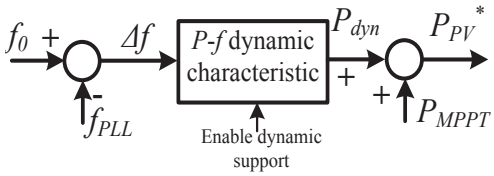

Fig.3. Block diagram of PV Frequency controller

rotating frames at -5ω (negative sequence) and 7ω (positive sequence) are employed. The converted current signals are provided to two integral controllers with the corresponding gains of K_{h5} and K_{h7}. The obtained compensation voltages are then added to the main *dq* VSC reference voltages.

When the energy storage system is connected to the VSC DC-link the battery acts as an energy buffer to balance the power between the PV production and the VSC output requirements. By this way the VSC output power is decoupled from the PV available power and, therefore, achieving a better control of the PV power

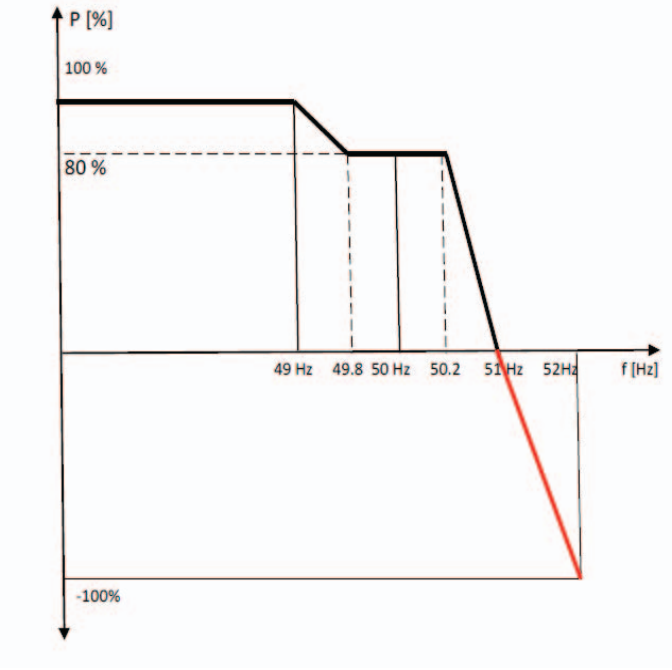

Fig. 4. Dynamic Frequency characteristic of the PV power plant

plant. In this paper, this characteristic is used to provide a certain level of support for the MG frequency.

When the support is enabled, the battery energy storage system is controlled to maintain the DC-link voltage constant by absorbing or injecting power by means of the bidirectional DC-DC converter. For a better assessment of the system performance, the conventional operation case of the PV power plant (i.e. without integrated storage) is also included in Section IV. In this case, the DC-link voltage is no longer regulated by the battery system, but by the internal VSC control.

B. Frequency Control

For the purpose of PV power plant participation in the MG frequency control process, a frequency controller is developed with the block diagram shown in Fig. 3. The frequency deviation Δf from the reference value f_0 – which may be fixed or controlled by the MG central controller – is used to determine the active power reference according to a predefined P-f characteristic. The signal P_{MPPT} comes from the MPPT block, which is not detailed in the current paper.

In order to analyse the proposed PV plant response to the frequency changes, for the simulations presented in section V an aggregate dynamic MG model is developed, based on the transfer function from (3) to represent the primary frequency control process, in per units (p.u.) [18].

$$G_{MGf}(s)=\frac{\Delta f_{MG}}{\Delta P}=\frac{1+sT_R}{2Hf_0T_Rs^2+(DT_R+2Hf_0)s+D+\lambda_{MG}} \tag{3}$$

where: Δf_{MG} is the MG frequency deviation; ΔP is the active power disturbance; T_R represents the composite time constant of the primary frequency control of the MG; λ_{MG} is the composite power-frequency characteristic of the MG; H is the inertial time constant of the MG; D is the load damping coefficient; f_0 is the initial steady-state frequency.

The active power-frequency characteristic is inspired from the existing PV grid code standards (Romanian grid code was targeted), being adapted for the required operation in MGs. As Fig. 4 illustrates, this characteristic is based on a 20 % reserve of the inverter when the frequency falls within normal operation range. Featuring an enhanced active power control due to the integrated storage, the characteristic can be expanded to the bottom quadrant also (i.e. P<0 – absorbing active power from MG). Therefore, the system can react to both signs of the frequency deviation. To be mentioned that, the current paper does not cover the cases when the battery reaches its state of charge (SOC) limits and when the system cannot longer operate as described. This aspect is reserved for future studies.

In order to highlight the proposed system behaviour in comparison with the conventional PV operation mode, two methods of generating the active power reference are used. In the first case a fixed reference value is used (i.e.

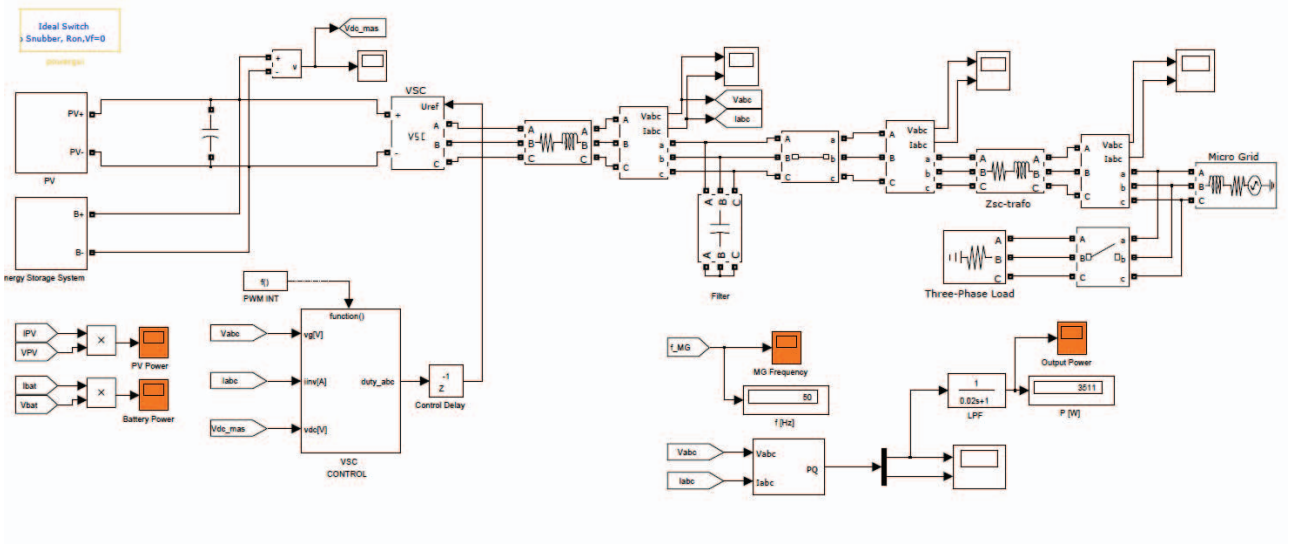

Fig. 5. Simulink block diagram Simulink of the studied system

provided by P_{MPPT}), while in the second case the dynamic frequency support is enabled.

Voltage regulation can also be provided through exchange of reactive power control [21], but in this case the reactive power reference is set to zero (Q_{PV}^{*}=0) in order the VSC to operate at unity power factor.

IV. Simulation Results

The PV system presented in Fig. 1 is modelled in Matlab/Simulink, and the main simulations of interest are discussed hereinafter. Fig. 5 presents the Simulink diagram of the PV inverter connected to the MG and main system parameters are presented in Table I. The VSC used here is a 5 kW three-phase inverter, sized to support the PV system above and to supply a 5 kW load connected to the MG. As for the simulation of the MG, is used a dynamic MG model in Simulink. The dynamic characteristic of the frequency presented in Fig. 4 is implemented in Simulink by means of a look-up table function. The MG model is developed according to expression (3), the frequency changing according to the active power balance in the MG. By this way, it is possible to analyse and optimize the PV power plant response during dynamic events in the MG.

In order to highlight the support capabilities of the studied system, the presented analysis includes the following operating cases: with and without dynamic support from the PV power plant, applied for different irradiation values and one more case, in which are applied the above conditions, but without battery support. There are three operating cases. In the first case there is a fixed value for the irradiation (G=1000W/m^2) and two assumptions with and without dynamic support, while in the second case the irradiation drops to a lower value (G=500W/m^2) in order to simulate a real PV operating condition also with the same assumptions. In the third case there are the same aforementioned conditions but without using the battery support.

The measurements include the MG frequency and the main active powers in the system (i.e. PV string, battery and VSC). For all cases, the MG is considered initially at steady-states with f_0=50 Hz.

As Fig. 6 shows, at t=2s when the load is connected, the frequency decreases rapidly to 48.72 Hz without dynamic support and to 48.86 Hz with dynamic support. After the primary frequency control is finished in about three seconds after the disturbance occurred, the frequency is restored in both cases to the rated value of 50Hz. Regarding the system active power flow, as shown in Fig. 7, without support the VSC output power has a small reaction to the MG frequency deviation. All the powers remain constant and the battery block is charged. The output power is constantly around 5000 W, after the load is switched on. With dynamic support, the PV power remains unchanged at around nominal value with a fluctuation after 2 second when the load is switched on. The VSC output power changes according to the characteristic from Fig. 4, increasing from 4000 W up to around 5000 W when the load is switched on, and again at 4000 W after that. During this time, the battery provides the balance of around 1250W between the PV and VSC power. This difference is smaller when the system operates without dynamic support and higher with dynamic support, the reason being the imposed operating characteristic of the frequency dynamic control for the VSC with power reserve, as described in section III.

TABLE I.
The Main System Parameters

Parameters	Values
VSC rated output power	5 kW
DC link voltage	650 V
Battery voltage	48 V
VSC output filter inductance and capacitance	3.1 mH; 10 µF
MG rated frequency (f_0)	50 Hz
MG time constant of the primary frequency control (T_R)	0.1 s
MG inertia constant (H)	1 s
MG damping factor (D)	2 %
MG power frequency characteristic (λ_{MG})	20 kW/Hz

In the second studied case, the PV irradiation changes from G=1000 W/m^2, to 500 W/m^2 at t=4s. For a better comparison these tests are accomplished for two operating conditions, i.e. without dynamic support and with dynamic support. As shown in Fig. 8, the frequency starts from the 50 Hz and after 2 seconds when the load is connected, it drops to 48.72 Hz without dynamic support, while with dynamic support being limited to 48.86 Hz. It should be mentioned that the frequency response is similar to the case presented in Fig. 6, since the integrated battery energy storage system ensures the power balance on the DC-link side of the VSC and, therefore, the VSC maintains its power response capability regardless of the PV production. As shown in Fig. 9, without dynamic support the PV power is constant around nominal value. After 4 seconds when the irradiation changes, the PV string power drops proportionally to 2000 W. However, due to the integrated energy storage system, the VSC output power is not affected, because during this time, when the irradiation drops the battery provides the balance between the PV and VSC power with a small fluctuation in both cases. The VSC output power being higher than the PV production, the battery provides the difference and starts discharging. Similar to the previous case, the balance is lower when the support is enabled in contrast to the operation without support. As a consequence, the MG frequency is undisturbed by the PV string power reduction at t=4s, as illustrated in Fig. 8.

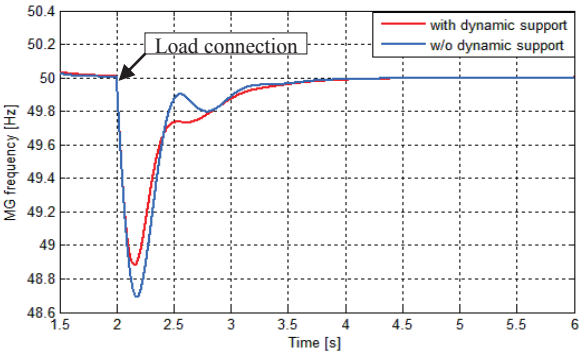

Fig.6. MG frequency for G=1000 W/m^2 without and with dynamic support.

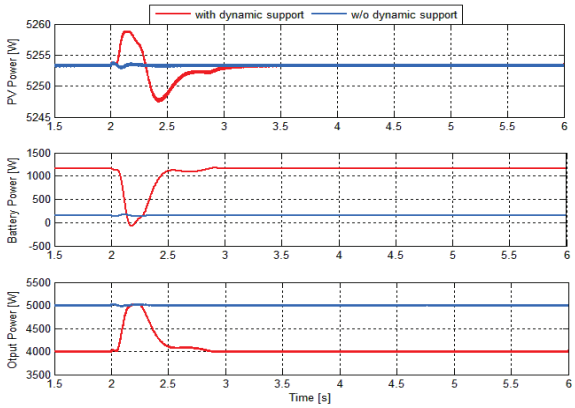

Fig.7. PV power, Battery power, Output power for G=1000 W/m^2 without and with dynamic support.

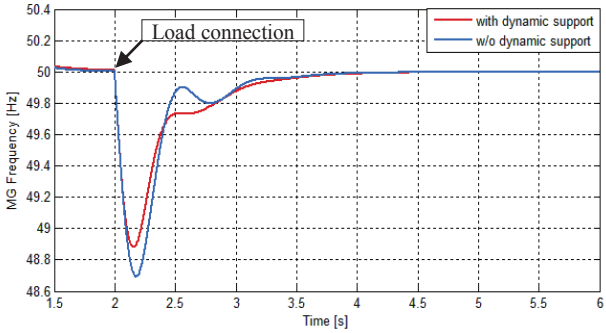

Fig.8. MG frequency for G=1000 W/m^2 and G=500 W/m^2 without and with dynamic support and with integrated battery.

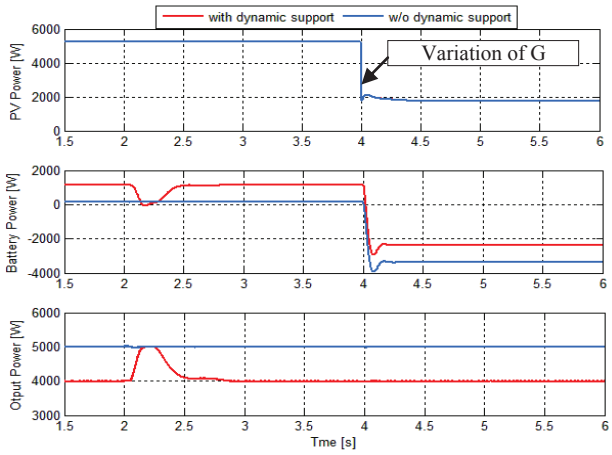

Fig.9. PV power, Battery power, Output power for G=1000 W/m^2 and G=500 W/m^2 without and with integrated battery.

In the third studied case, the PV irradiation changes from G=1000 W/m^2, to 500 W/m^2 at t=4s as in the previous case, but now the battery is removed from the DC-link. In order to compare this case with the other two above, these tests are accomplished in the same operation conditions, without dynamic support and with dynamic support. As shown in Fig. 10, frequency starts from the 50 Hz, and after 2 seconds when the load is connected, the frequency starts declining to 48.72 Hz without dynamic support and to 48.86 Hz with dynamic support. At around t=4s the frequency is restored to the rated value in both cases, i.e. with and without dynamic support. However, after t=4s, when the irradiation changes to 500 W/m^2 the MG frequency is dropping to 49.4 Hz without dynamic support, while being limited to around 49.7 Hz when the support is enabled. After 5.8 seconds the frequency is brought back to 50 Hz in both cases.

As shown in Fig. 11, without dynamic support the PV power is at a constant value around the nominal value of 5000 W, while in the other case the PV power changes from 4000 W to 5000 W after 2 seconds when the load is switched on and again at 4000 W. The output power is 5000 W without dynamic support, whereas with dynamic support being maintained at 4000 W, according to the characteristic from Fig. 4, with a minor fluctuation when the load is switched on.

After 4 seconds, when the irradiation changes, the PV string power drops proportionally to the irradiation to approximately 1700 W and remains constant in both cases, i.e. with/without dynamic support. However, due to the lack of integrated energy storage system, the VSC output power now follows the PV string production and, therefore, it can no longer sustain the MG frequency, until the MG frequency is stabilized again after 5.8 s at 50 Hz. As a consequence, the irradiation change perturbs the MG and the frequency drops according to the PV active power decrease (i.e. 4000 W), but this perturbation is limited due to the dynamic characteristic of the frequency when the system is working with dynamic support.

Further improvements are under study, one of these consisting in adapting the PV power plant response capability according to the battery state-of-charge. Enhancing the frequency controller to respond to the rate-of-change-of-frequency is another improvement taken into consideration.

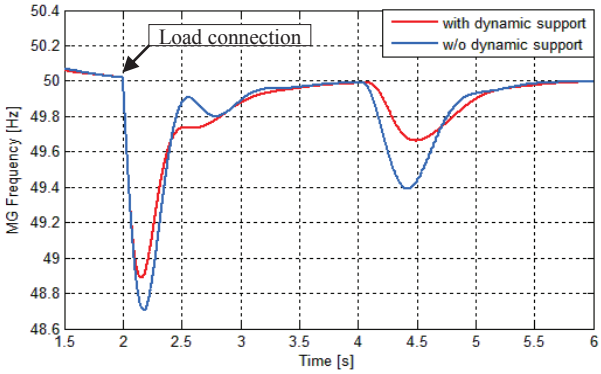

Fig.10. MG frequency for G=1000 W/m^2 and G=500 W/m^2 with and without dynamic support and without integrated battery.

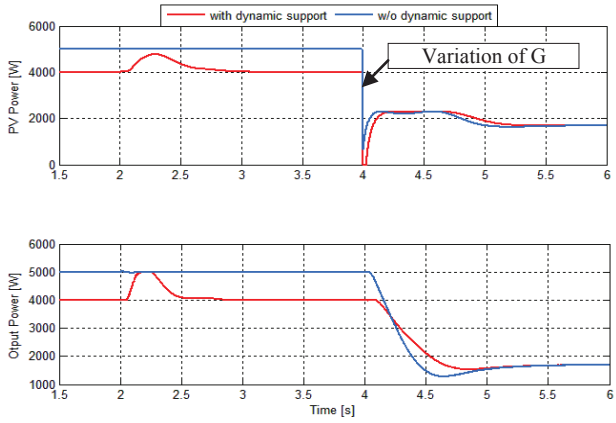

Fig.11. PV Power, Output power for G=1000 W/m^2 and G=500 W/m^2 without and with dynamic support and without integrated battery.

V. CONCLUSIONS

The paper has presented a solution for dynamic support of frequency in microgrids (MGs) by means of photovoltaic (PV) power plants. In order to improve the PV system control and power reserve, an energy storage system is integrated into the structure of the PV power plant. The PV response to frequency deviations is adapted from the existing Romanian grid code, a modified *f-P* characteristic being developed according to the system characteristics. The simulation results have clearly shown that, as long as the battery storage system operates in normal conditions (i.e. without storage limitations), the considered PV system is able to improve the MG frequency response and for sure the dynamic frequency support according to existing power reserve, ensures an increased stability of the entire MG output power. Regarding the PV power it was demonstrated that, according to irradiation values, the battery compensates for the difference between the PV string production and the imposed PV plant output power according to the frequency controller characteristic. The case without integrated energy storage system was also analyzed, the results showing that the PV power plant can provide a certain level of support according to its power reserve operation, which depends on the irradiation level.

Received on July 17, 2016
Editorial Approval on November 15, 2016

REFERENCES

[1] N.W.A. Lidula, A.D. Rajapakse, Microgrids research: A review of experimental microgrids and test systems, Renewable and Sustainable Energy Reviews, Volume 15, Issue 1, January 2011, Pages 186-202.

[2] N.Hatziargyriou, "Microgrids: Building Blocks of the Smart Grid", IEEE PES ISGT Europe, Berlin, Germany, 14-17Oct., 2012.

[3] S. Parhizi, H. Lotfi, A. Khodaei and S. Bahramirad, "State of the Art in Research on Microgrids: A Review", IEEE Access, vol. 3, pp. 890-925, 2015.

[4] M. Rezkallah, S. Sharma, A. Chandra and B. Singh, "Hybrid standalone power generation system using hydro-PV-battery for residential green buildings", 41st Annual Conference of the IEEE Industrial Electronics Society (IECON), Yokohama, pp. 003708-003713, 2015.

[5] K. F. Krommydas and A. T. Alexandridis, "Modular Control Design and Stability Analysis of Isolated PV-Source/Battery-Storage Distributed Generation Systems", IEEE Journal on Emerging and Selected Topics in Circuits and Systems, vol. 5, no. 3, pp. 372-382, Sept. 2015.

[6] H. Mahmood, D. Michaelson and J. Jiang, "A Power Management Strategy for PV/Battery Hybrid Systems in Islanded Microgrids", IEEE Journal of Emerging and Selected Topics in Power Electronics, vol. 2, no. 4, pp. 870-882, Dec. 2014.

[7] S. Adhikari and F. Li, "Coordinated V-f and P-Q Control of Solar Photovoltaic Generators With MPPT and Battery Storage in Microgrids", IEEE Transactions on Smart Grid, vol. 5, no. 3, pp. 1270-1281, May 2014.

[8] H. Mahmood, D. Michaelson and J. Jiang, "Strategies for Independent Deployment and Autonomous Control of PV and Battery Units in Islanded Microgrids", IEEE Journal of Emerging and Selected Topics in Power Electronics, vol. 3, no. 3, pp. 742-755, Sept. 2015.

[9] Y. Guan, J. C. Vasquez, J. M. Guerrero, Y. Wang and W. Feng, "Frequency Stability of Hierarchically Controlled Hybrid Photovoltaic-Battery-Hydropower Microgrids", IEEE Transactions on Industry Applications, vol. 51, no. 6, pp. 4729-4742, Nov.-Dec. 2015.

[10] Y. Yang, F. Blaabjerg and H. Wang, "Constant power generation of photovoltaic systems considering the distributed grid capacity", IEEE Applied Power Electronics Conference and Exposition (APEC), Fort Worth, TX, pp. 379-385, 2014.

[11] A. Sangwongwanich, Y. Yang and F. Blaabjerg, "High-Performance Constant Power Generation in Grid-Connected PV Systems", IEEE Transactions on Power Electronics, vol. 31, no. 3, pp. 1822-1825, March 2016.

[12] J. Quesadaa, R. Sebastiánb, M. Castrob, J.A. Sainz, "Control of inverters in a low voltage micro-grid with distributed battery energy storage. Part I: Primary control", Electric Power Systems Research, vol. 114, pp. 126–135, Sept. 2014.

[13] S. Gaurava, C. Birlaa, A. Lambaa, S. Umashankara, S. Ganesanb, "Energy Management of PV - Battery based Micro-grid System", Procedia Technology, vol. 21, pp. 103 – 111, 2015.

[14] F.M. Uriarte, C. Smith, S. VanBroekhoven, R.E. Hebner, „Micro-grid Ramp Rates and the Inertial Stability Margin", IEEE Transactions on Power Systems, vol.30, no.6, pp.3209-3216, Nov. 2015.

[15] J. G. de Matos, F. S. F. e Silva and L. A. d. S. Ribeiro, "Power Control in AC Isolated Microgrids With Renewable Energy Sources and Energy Storage Systems", IEEE Transactions on Industrial Electronics, vol. 62, no. 6, pp. 3490-3498, June 2015.

[16] J. M. Guerrero, M. Chandorkar, T. L. Lee and P. C. Loh, "Advanced Control Architectures for Intelligent Microgrids—Part I: Decentralized and Hierarchical Control", IEEE Transactions on Industrial Electronics, vol. 60, no. 4, pp. 1254-1262, April 2013.

[17] R. Teodorescu, M. Liserre, P. Rodriguez, "Grid Converters for Photovoltaic and Wind Power Systems", IEEE-Wiley, 2011.

[18] I. Serban, R. Teodorescu, C. Marinescu, "Energy storage systems impact on the short-term frequency stability of distributed autonomous microgrids, an analysis using aggregate models," IET Renewable Power Generation, vol. 7, no. 5, pp. 531-539, Sept. 2013.

[19] Tang X, Deng W, Qi Z. "Investigation of the Dynamic Stability of Microgrid", IEEE Transactions on Power Systems, vol. 29, no.2, pp: 698-706, 2014.

[20] D. Munteanu, C. Marinescu, I. Serban, L. Barote, "Control of PV Inverter with Energy Storage Capacity to Improve Microgrid Dynamic Response" ICATE- Craiova, Oct. 2016.

[21] B. I. Craciun, D. Sera, E. A. Man, T. Kerekes, V. A. Muresan, R. Teodorescu, "Improved voltage regulation strategies by PV inverters in LV rural networks," 3rd IEEE International Symposium on Power Electronics for Distributed Generation Systems (PEDG), Aalborg, 2012, pp. 775-781.